

Aging Comparison between Two Battery Cells LiFePO_4 and $\text{Li}(\text{NiMnCo})\text{O}_2$ in Vehicle to Grid Operations

Timo A. Lehtola and Ahmad Zahedi

Abstract—The objectives of this study are to show how significantly Vehicle to Grid (V2G) systems are affecting the lifetime of the electric vehicle batteries. In V2G use, electric power is flowing from the power grid to the electric vehicle batteries and from the batteries to the power grid. Using direct real-time control of the grid operator, batteries are charged, providing V2G balance and frequency regulation to the grid. In this research, two different types of cells were used to investigate how the V2G charge limits affect the battery lifetime. Battery aging model is previously used to calculate lifetime and cost of V2G use. This research increases knowledge by comparing two different types of battery cells. Batteries are expensive and lifetime increase is one solution to reduce costs. The results indicate that battery management can optimize battery use with longer battery life. The main goal of the manuscript is to receive a longer battery life. As a result, lifetime was calculated at four years for A123 Systems™ cells and 18.27 years for Sanyo's™ cells. This research connects measurement data, driving data, proposed V2G use to existing battery cycle aging model. For satisfying the scheduled charging, the V2G control is switched to a smart charging control. The V2G concept is found to be as an extension of the smart grid system allowing electric vehicles to be able to inject electricity into the electricity network, acting as distributed generating systems or battery storage systems. As smart charging is an important part of electric vehicle penetration, V2G may provide an important bonus for smart charging procedures. The proposed topic is interesting and worthy of investigation since the impact of V2G operations on battery durability plays an essential role for the convenience of vehicle owners in supporting the electricity network with this kind of ancillary services. Main findings are lifetime reduction is decreased in V2G operations and a lifetime can be extended.

Index Terms—Cycle life, electric vehicle, Li-ion battery, smart charging, vehicle to grid.

I. INTRODUCTION

In V2G systems, Electric Vehicle (EV) batteries provide electricity for EV propulsion and improve the power grid stability. These dual uses of batteries increase the degradation of the batteries. The State of Charge (SoC) express the level of charge in the battery cell. Operators affect the battery lifetime by keeping the batteries stored at different SoC levels. Battery's lifetime needs to be improved to increase battery efficiency and reduce battery wear. Battery wear needs to be considered as a part of the economic evaluation. EV operators have battery wear cost due to V2G operations. EV operators consider V2G cost and battery replacement as a

part of the operational cost because of a decreased battery lifetime.

The Lithium-ion (Li-ion) battery model indicates that intelligent charging and V2G operations reduce the average SoC, which slows down battery aging. In V2G use, battery lifetime was considered until it reached 80% of the original battery capacity. This means that fully charged 100% SoC battery cell has 80% capacity. The objective of this research is to increase the lifetime of batteries in V2G operations. Using the battery cell aging model we calculate how many years of battery cells last in V2G operations in normal driving patterns. Optimal charging procedure chooses optimal charge limits according to a driving distance of that day.

Cycling tests for LiFePO_4 batteries showed that LiFePO_4 battery cells are not so sensitive to the Depth of Discharge (DoD) as many other Li-ion batteries [1]. This means that EV can use a higher proportion of batteries and use smaller capacity batteries. Battery capacity refers to the maximum capacity that the cell can deliver from a full discharge process. The capacity fading after cycles should be calibrated by standard capacity tests, those under standard rate and temperature. The experiments and the Reference Performance Tests (RPT) has been conducted on a LiFePO_4 ANR26650M1-A™ cell manufactured by A123™ Systems providing a tool for lithium plating detection [2]. Experiments with $\text{Li}(\text{NiMnCo})\text{O}_2$ battery cells showed that the lowest degradation was when SoC was near 50% [3]. V2G cycles between 47.5 and 52.5% SoC allowed the highest lifetime of 8,500 equivalent full life cycles, and the full area cycles allowed the lowest lifetime of 440 cycles until reaching 80% of the original cell capacity [3]. Equivalent full cycles mean partial charges, which charge maximum range to the batteries. For example, in 240 km range, electric vehicles 200 km and 40 km partial charges develop one equivalent full cycle.

To ensure a prolonged lifetime, EV batteries should recharge soon after battery remaining charge 50% SoC or less. In turn, the low charge level will cause deep cycles, increasing battery aging. During cycle life tests, after battery cells reached 80% of the original battery capacity, battery cells began to have unexpected deaths [3]. That implies that battery cells are not trustworthy after reaching 80% of the original battery capacity. However, batteries can be used after reaching 80% on second-life battery applications. Battery storage tests showed that empty batteries had the smallest capacity fade and full batteries had the strongest capacity fading during 400 days test [3]. An aging test with $\text{Li}(\text{Ni}_{1/3}\text{Mn}_{1/3}\text{Co}_{1/3})\text{O}_2$ illustrated that the best average SoC area is 30-50% [4], which is slightly under the optimal 50% SoC for $\text{Li}(\text{NiMnCo})\text{O}_2$ batteries [3].

Here is a list of common EV battery chemistries. EV

Manuscript received June 14, 2019; revised August 26, 2019. This work was supported in part by the College of Science and Engineering and the Graduate Research School, James Cook University, Australia.

T. A. Lehtola and A. Zahedi are with the James Cook University, Townsville, QLD 4814, Australia (e-mail: timoantero.lehtola@my.jcu.edu.au, ahmad.zahedi@jcu.edu.au).

battery chemistries have different performance characteristics, limitations, and development breakthroughs. EV battery materials are Lithium Cobalt Oxide LiCoO_2 (LCO), Lithium Nickel Cobalt Manganese oxide $\text{LiNi}_x\text{Co}_y\text{Mn}_z\text{O}_2$ (NCM or NMC), the common form $\text{LiNi}_{1/3}\text{Mn}_{1/3}\text{Co}_{1/3}\text{O}_2$, Lithium Nickel Cobalt Aluminum oxide $\text{LiNi}_{0.8}\text{Co}_{0.15}\text{Al}_{0.05}\text{O}_2$ (NCA), Lithium Iron Phosphate LiFePO_4 (LFP), and Lithium Titanium Oxide (LTO). Panasonic™ batteries for Tesla™ EVs use NCA chemistry. Other chemistries include Lithium Manganese Oxide LiMnO_2 (LMO), $\text{Li}_2\text{Mn}_2\text{O}_4$ (also LMO), Lithium Cobalt Phosphate LiCoPO_4 (LCP), Lithium Iron Fluorosulfate LiFeSO_4F (LFSF), and Lithium Titanium Sulfide LiTiS_2 (LTS). The list continues with cathodes LiNiO_2 (LNO), $\text{Li}(\text{Ni}_{0.5}\text{Mn}_{0.5})\text{O}_2$ (NMO), LiMnPO_4 (LMP), $\text{LiNi}_{0.5}\text{Co}_{0.5}\text{PO}_4$ (NCP), $\text{LiMn}_{1/3}\text{Fe}_{1/3}\text{Co}_{1/3}\text{PO}_4$ (MFCP), and $\text{Li}_3\text{V}_2(\text{PO}_4)_3$ (LVP).

Battery cell wear decreases battery capacity, increases inner resistance, increases power loss, and causes a variation in impedance spectra. Battery cell wear depends on temperature, DoD, and charging and discharging power [5]. Battery temperature control is a vital part of EV battery management systems. The aging rate for battery cells doubles when the cell temperature rises by 10 °C [4]. TABLE I lists several aging tests, which have been carried out with different cathode materials.

TABLE I: CONSIDERED CONTEMPORARY CYCLE LIFE STUDIES

Positive electrode (cathode) material	Cycle life studies*
LiMn_2O_4	[6]
$\text{Li}(\text{NiMnCo})\text{O}_2$ or $\text{Li}(\text{Ni}_{1/3}\text{Mn}_{1/3}\text{Co}_{1/3})\text{O}_2$	[7]
LiCoO_2	[6]
LiNiO_2	
$\text{LiNi}_{0.8}\text{Co}_{0.15}\text{Al}_{0.05}\text{O}_2$	[8]
$\text{LiNi}_{0.8}\text{Co}_{0.2}\text{O}_2$	
LiFePO_4	[6, 8]
$\text{LiNi}_{0.5}\text{Mn}_{1.5}\text{O}_4$	

*For more details, see the references.

Aging tests detected capacity fade as well as an increase of inner resistance. The main reason may be thermal processes, which were linear with time. An article [6] presented developed improved health monitoring methods universal capacity model based on the charging process was developed. In addition, the anode impedance increased manganese dissolution on carbon anodes. External aging reactions accelerate the aging including Solid Electrolyte Interface (SEI) growth, lithium material loss, as well as lithium plating. The aging model studied the path dependency of EV battery cell degradation and aging and synthesized various battery-aging scenarios in regard to battery degradation methods, such as loss of active electrode material, loss of lithium inventory, degradation kinetics, increased polarization resistance, the influence of parasitic phases on the electrical properties, and lithium plating. After 120 days of operation, cells were tested and the internal resistance increase was lower than 1%. The explanation could be lithium insertion or extraction processes in electrode particles that in turn may cause mechanical fracture of active particles. Battery degradation model [7] was presented since the model can be smoothly integrated into the energy simulation and

presents an estimation for the battery cell aging. Generally can be stated that EV technology is a promising technology for future transportation [9].

Aging tests described incomplete stripping of lithium as an effect of the SEI growth. The SEI growth increases an effective loss of lithium metal on model substrates. The main reason for cell capacity degradation is the loss of active lithium due to SEI growth and electrode degradation. An article [10] investigated the calendar aging of Li-ion battery cells and cycle aging for several temperatures and SoC levels. They obtained predictions from the capacity model and validated the model with measurements. The obtained data were from cycle aging measurements, with an estimation of capacity loss.

Battery capacity degradation rate influences the driving distance and decreases the discharge capacity level because of ancillary services. This understanding enables to establish a quantitative physical model. This model describes the cell aging process with a capability to accommodate variation in battery cell aging due to power pulses and thermal cycling. An alternative approach would be that increased capacity superimposes SEI formation as proposed in an article [11]. For battery aging prediction, many aging characteristics have been accounted for. These characteristics include temperature, storage voltage, time, cycle depth, SoC, current rate, and charge throughput [11]. The calendar and cycle life experimental tests indicate that lower temperatures result in a longer lifetime. The characteristics are SoC, capacity, impedance, power level, State of Health (SoH), and lifetime. The challenge is that most of battery cell parameters, including, battery cell capacity and impedance characteristics, and varies significantly due to aging. The metallic lithium plating on the electrode is the main reason of safety hazard and influences to the aging.

The change in current rate changes the capacity fade. The higher rates of current draws accelerated the deterioration of Li-ion electrodes. A capacity analysis uses SoC to estimate the capacity fade. However, it is challenging to determine the SoC precisely. In addition to capacity and resistance characteristics, aging studies focus also on equivalent circuit analysis in cycle aging and in calendar aging. However, increased charge voltage increases the rate of capacity degradation. The capacity degradation rate is independent of the SoC when SoC is lower than 50%. Therefore, a battery cell aging decreases battery energy capacity [12]. Stack stress evolution is a dynamic quantity during battery cell aging. As a result of electrode charging strains stack stress fluctuates with SoC and gradually accumulates over the cell aging. The capacity fade occurs after an extended cycle test. The capacity fade and the internal impedance increase during extended cycle test increasing changes in the material structure and phase of the cathode. Aging tests showed the influence of the discharge current, AC current waveform shape, AC current frequency, and root mean square current amplitude on battery aging [13].

In a hybrid EV study, a load profile maintained 60% SoC. The capacity degradation was included in an empirical cycle aging model [8]. However, this empirical aging model was not able to revive the degradation mechanism.

In LiFePO_4 aging tests, the capacity decreased faster with the temperature than with the SoC. The main reason for the

aging process is the loss of active lithium inventory because of SEI growth. SoC, temperature, and It-rate contribute to battery cell aging and are included in the LiFePO₄ cell aging model [14]. Loss of active lithium is the main reason for battery cell aging. Firstly, metal ions on anode have a reaction with electrolyte and dissolve in the electrolyte. Secondly, electrolyte reacts with the cathode. Finally, SEI film reduces active Li-ions in the cathode. The SEI growth on electrode surfaces causes particle disconnections. This, in turn, increases material resistance and causes capacity degradation. Experiments showed an increase in LiFePO₄ cell inner resistance [14]. A degradation process for LiFePO₄ cells starts with the loss of active lithium inventory. The following development is a combination of loss of active lithium inventory, loss of active material, and degradation of reaction kinetics. The loss of active lithium inventory is the main reason for aging during the first phase of the degradation process. Thus, the loss of active material in anode surface accelerates near the End of Life (EoL) for cycle life experiments. The lifetime of LiFePO₄ cells is longer at low charging and discharging rates than at high charging rates. Unwanted lithium plating is only observed when battery cells are charged and discharged in a narrow SoC window. Factors for battery lifetime include ambient temperature, charging and discharging rates as well as charging and discharging cut-off voltage as the input stresses. The influence of ambient temperature refers to the Arrhenius method whereas the influence of electrical factors refers to an inverse power law relationship [14]. They analyze the influence of the battery cell life based on the sensitivity of factors of the life model. A diagnostic technique to indicate an SoH for Li-ion cells analyses measured voltage and current signals. The degradation process correlates to the special materials on the battery cells and to the manufacturing method of the cell. A battery-aging model investigates and considers the contribution of temperature, cycle rate, and DoD. An article [1] analyses the business value of V2G operations for load management in a power grid. The received benefits need to exceed the cost of V2G operations. Considered benefits of V2G operations are, for example, providing peak power management or spinning reserve services. Considered the cost of V2G operations are EV battery capacity fade, V2G electronics and communication infrastructure, and energy production losses. A real-time distributed energy management may increase profitability [15] of V2G operations. The energy management also maximizes each producer's gains by selling its excess energy not only to the utility companies but also to neighbors at an optimal selling price, which will motivate the local renewable energy investment [15]. In cell power performance fade, plated lithium loses its conductive connection to graphite by isolation. The lithium lost may enhance the growth of the SEI layer, which deteriorates ionic kinetics in the anode materials. Like this, in turn, enhances the lithium plating. This is a circle process, which may cause a loss of battery electrolyte, because of a steady decomposition leading to the end. The high ambient temperature and calendar aging induce extra battery aging and therefore, the main degradation process, loss of lithium, changes to a combined loss of lithium material and loss of active lithium. The loss of active lithium accelerates the battery cell performance fade. The

combination of calendar and cycle aging covered a wide range of combinations to form a cost-effective methodology for reliable lifetime estimation [16]. The shallower the DoD, the more energy can be cycled before the cell reaches EoL. LiFePO₄ chemistry provides a long calendar aging [17]. The cycle aging will reach 8,000 cycles at room temperature. Power degradation under normal EV cycles is between very low, 3.27–5.59%. The reduction of EV range is mainly based on capacity fade rather than power degradation. Li-ion cells experience calendar aging and cycle life aging. The monitoring system for performance degradation can track the capacity fade and increase the inner resistance. In calendar and cycle aging, inner resistance increases because of contact losses and formation of resistive surface film behavior. Loss of Li-ions and active electrode material can influence capacity fade. Calendar and cycle aging depends on battery cell chemistry and operational conditions. Operational conditions for calendar aging are temperature, SoC, and time. Operational conditions for cycle aging are temperature, SoC, cycle number, as well as charge and discharge voltage. Some aging factors come from the power grid, for example, peak current demand. These variables interact with each other's forming a complicated process for aging. Therefore, models can estimate aging and experimental tests provide figures that are more realistic. Interactions may be difficult to understand and quantify [18].

For Li(Ni_{1/3}Mn_{1/3}Co_{1/3})O₂ tests, the lowest test temperature was 25 °C and the lowest test storage charge was 20% SoC, revealing the longest battery lifetime expectations [11]. Calendar aging for Li(NiMnCo)O₂ showed that empty cells survived longest and cells cycled around 50% SoC offered the longest lifetime [3]. EV batteries have similar lifetime expectations; however, differences come from technology, battery management, producer, and battery model. Several cycle aging measurements and cycle aging models exist. Some of these use daily driven patterns and connect V2G operations to that model. In addition, some studies calculated EV battery lifetime in years or calculated lifetime driving range. Table II lists five methods used for cycle aging studies.

TABLE II: CONSIDERED METHODS OF THE PROPOSED APPROACH IN CONTEMPORARY CYCLE LIFE STUDIES

Study method	Cycle life studies*
Cycle life measurements	[6, 8, 10]
Cycle life models	[6, 8, 10, 19]
Daily driven patterns	[10, 19]
Connect V2G use to that model	[8, 10]
Calculated EV battery lifetime in years or calculated lifetime driving distance	[8, 10]

*For more details, see the references.

Cycling experiments with the LiNi_{0.5}Mn_{1.5}O₄ electrodes involved irreversible phenomenon: the measured charge capacity was higher than the available discharge capacity [20]. Note, however, that cycling rate was It/16, which is lower than normal cycling rate for the commonly available EV chargers rates. Therefore, slow charging with high voltage can cause unwanted anode reactions and increase anodic currents. The inner resistance rise and degradation of capacitance parametrization factors rely on the operational position of the EV battery cell. Therefore, inner resistance rise and degradation of capacitance depend on temperature,

time, SoC, power demand, and cell aging. A study [21] carried out experimental tests on battery cells stressed with different charging and discharging rates. These experiments estimated SoH and consequently the effects due to cell aging. Cell aging studies reveal that either the DoD increase from 20 to 40% or the temperature increase from 25 to 45 °C, have a small impact on cell degradation and end of voltage. The discharge rate was $I_t/3$ [22]. However, a simultaneous increase in DoD and temperature significantly increases degradation. In cycle aging performance tests, the cells subjected to a higher temperature do not experience high power degradation, which is an unexpected result. However, cells show increased variability in degradation when cells are cycled at the same temperature [23]. An article [24] studies the lifetime of the battery energy storage systems under various assumptions. However, the missing point is feasibility due to the arbitrary choice of battery recharge thresholds to trigger corrective measures. Battery management can enhance the lifetime of batteries by choosing optimal charging strategies. Significant barriers to EV technology exists, such as the demand for driving range and the demand for EV charging stations, that still prevents the widespread use of EVs [19]. In our previous work, empirical battery cycle aging model for V2G application including daily driven patterns was used to calculate annual battery wearing cost [10].

Table III shows the comparison of the considered methods with contemporary literature regarding cycle life models and V2G operations. Majority of the research works cover only measurements and/or models. Typical missing parts are daily driven patterns, years or driving distance, and V2G operations. This research connects battery cell aging measurements, vehicle driving distance data, and V2G operations to the developed cycle aging model. This model is an empirical battery cell cycle aging model developed in our previous work [10].

TABLE III: SALIENT FEATURES OF THE PROPOSED APPROACH IN COMPARISON WITH THE CONTEMPORARY CYCLE LIFE STUDIES

Considered methods*	Measurements	Models	Daily driven patterns	Years or driving distance	V2G
[12]	✓				
[6]	✓	✓			
[18]	✓		✓		
[19]		✓	✓		
[17]	✓	✓	✓		
[3]	✓	✓		✓	
[16]	✓	✓			✓
[1]	✓	✓	✓		✓
[8]	✓	✓		✓	✓
[10] [This paper]	✓	✓	✓	✓	✓

*For more details, see the references.

Considered methods cycle life measurements, cycle aging models, daily driven patterns, battery life in years, calculated lifetime driving distance, and the V2G connection was all covered in [25]. The aging model examined the degradation of battery cells. The loading behavior adapted various driving scenarios and charging schemes. V2G operations can provide peak shaving service for the power grid. The findings demonstrated that V2G operations reduced the battery cell

life due to the prolonged discharging and greater cycle depths in discharging. However, intelligent charging schemes may enhance battery life.

On the base of a large number of literature references, grid operators could perform V2G operations in the future through different aggregation schemes, which involve an agent and multi-agent logic. For this reason, the grid operators will probably avoid direct real-time control in the future. A large number of literature references presented battery cycle measurements and battery aging models. Only a few literature references discuss battery lifetime in years, calculate lifetime driving distance and provide V2G operations.

The research problem is that V2G operations decrease battery lifetime. The objectives of this study are to demonstrate how much V2G operations affect the lifetime of the batteries. Purpose of this study is to find an approach to enhance the lifetime of the batteries. This proposal used cycle life measurements and cycle life model for investigations. We connected daily driven patterns and V2G operations to that model and we calculated EV battery lifetime in years and lifetime driving distance. We obtained how much V2G operation reduced cycle lifetime and how much reduced lifetime cost for battery owner. We learned that annual driven distance, number of V2G cycles, and battery cost increased annual V2G cost. As seen in TABLE III, only three articles cover all considered methods measurements, cycle life models, daily driven patterns, calculating lifetime and driving distance and V2G operations. The contribution of this research is to connect all these considered methods to our battery cycle aging model. The model optimizes charging and discharging and calculates an approximation of a battery's life cycle. The novelty of this work in relation to similar work is the use of charge limits according to driving distance. This leads a great help for V2G battery management developers. We recommend utilizing this battery model for EV battery management systems to enhance the lifetime of battery cells.

An outline of this research is as follows. Section II provides a methodology. Section III discusses the configuration of the cycle aging model, its flexibility, and the possible extension of its application area. Section IV connects measurements to cycle aging model, presents and discusses the main outcome. Section V describes validation for the proposed model, in its initial and stochastic formulations. The same section presents the results and discusses the application of the proposed realistic model study. Finally, interpretation, discussion, and the conclusion summarizes the main results of the paper and offer some hints about possible future developments.

The flowchart shows the investigation procedure, Fig. 1. In the beginning, we had initial values of EV and batteries. From driving data, we received average driving distance. We decided to use four charge limits, which means four distances for charging range. As a result, we received equivalent full cycles. From measurement data, we received the cycle life of the batteries. We compared those to another measurement data. We chose a number of V2G cycles and received annual distance. We optimized cycle lifetime and received increased cycle lifetime for battery cells.

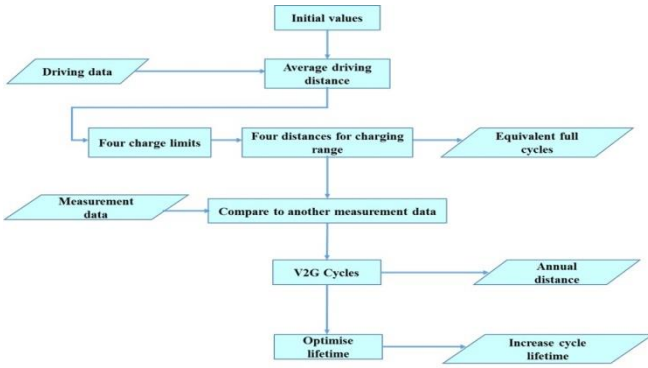


Fig. 1. The investigation procedure. Inputs are driving data and measurement data. Outputs are equivalent full cycles, annual distance and increase cycle lifetime.

II. METHODOLOGY

Accelerated battery cell aging data were collected from two different sources [3], [14] and were constructed in different ways. A123 Systems™ cells tests were carried out with two measurements at six different temperatures, five different DoDs, and four different It-rates. The total number of cycles per lifetime was recorded. Sanyo’s™ cells tests were carried out with several measurements: 35 °C, 1It current, and six different SoC levels. Battery capacity was kept at an average SoC of 50%. The aging level was recorded several times during measurements. The effects of different models (26650, 18650) were excluded from this study.

Real driving data were collected and demand for equivalent full cycles were recorded. V2G cycles drew 5% of battery energy in time and a total number of V2G cycles were from 12 to 32 cycles per day. Aging data showed a number of cycles during the lifetime. These lifetime cycles were transformed to driving distance using range information from BYD e6™ and Tesla Model S™ vehicles. As a result, the full driving distance was divided by average annual 20,000 km distance answering to question how many years batteries last in V2G operation.

III. CONFIGURATION FOR BATTERY MODEL

A. Details for Battery Model

Battery lifetime equations in this study were based on an earlier introduced model [10], which is implemented for the Engineering Equation Solver (EES). Contour plots were formed in EES. Vehicle information initial values were from Build Your Dreams (BYD) e6™ Battery Electric Vehicle (BEV). The range was 204 km and the battery capacity was 75 kWh. Battery cells were the A123 Systems’ ANR26650M1-A™ LiFePO₄ cells. The electric charge for these 26650 cylindrical cells was 2.2 Ah. Results were compared to Sanyo’s UR18650E™ Li(NiMnCo)O₂ cells. Vehicle information initial values were from the Tesla Model S™ BEV. The range was 500 km and battery capacity was 85 kWh. The electric charge for these Sanyo 18650™ cylindrical cells was 2.05 Ah. BYD e6™ and Tesla Model S™ have the range difference for similar battery capacity. One of the possible reasons may be that Tesla has an aluminum body. Measurements have been made to battery cells, not to the battery pack. This study does not take account

battery pack construction and its influence on the battery lifetime.

B. Annual Equivalent Full Cycles

Information about daily driven distances comes from the National Household Travel Survey (NHTS) [26]. According to the NHTS, Fig. 2 shows that 19%, 21%, and 16% of the drivers who participated in the national survey would travel 8 km, 24 km, and 40 km respectively on a daily basis, wherein total, 85% would travel up to 105 km. A number of cars were 179,484. Using NHTS data, the battery charging was divided into four different charge limits according to the traveling distances: 25, 50, 75, and 100 km. Battery lifetime is optimized by choosing the optimal charge limit. Data values for Fig. 2 are 19.42; 21.23; 16.30; 11.30; 8.18; 5.78; 4.22; 2.79; 2.14; 1.62; 1.30; 0.81; 0.78; 0.58; 0.45; 0.39; 0.29; 0.26; 0.13; 0.13; 0.16.

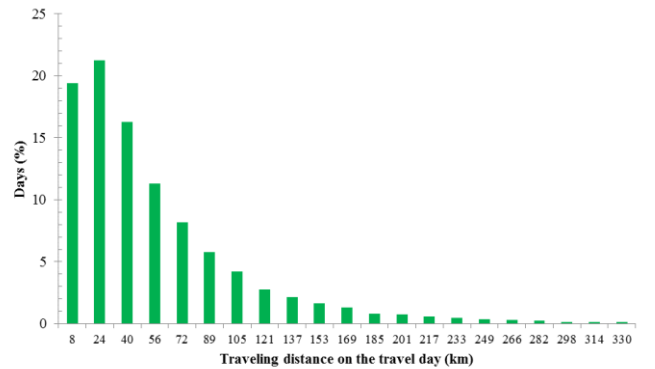


Fig. 2. Daily traveling distances. The distribution of the total driving distance on the travel day.

Full cycle means that the total range of 204 km was used. When batteries were charged and discharged partly, only a fraction of the total battery capacity was used. This charged distance was compared to the full range, called the equivalent full cycle. Several equations were used to calculate the lifetime and the cost of V2G use. Equations were implemented in EES software. The battery cell temperature used in the calculation is 35 °C and DoDs are 12, 25, 37, and 49%, corresponding four distances are 25, 50, 75, and 100 km. Equation (1) calculates equivalent full cycles per year

$$N_{acd} = \frac{D_{dd}}{D_{range}} \times N_d, \quad (1)$$

where D_{dd} is the daily distance drove, D_{range} is the driving range, and N_d is the number of annual driving days (TABLE IV). For example, a traveling distance of 8 km was done 71 days per year and the range was 204 km. Equation (1) gave an equivalent full cycle of 2.78, which means that the driven distance was 2.78 times 204 km. In that case, the shortest charge limit 25 km (DoD 12%) was enough to cover 8 km driving and only one charging was needed that specific day. Table IV shows real-life data adapted from Fig. 2.

Fig. 3 shows equivalent full cycles per travelling distance calculated from (1). The physical implication of (1) is degradation of batteries, because of travelling distance. One can notice that compared to Fig. 2, degradation is relatively higher at longer distances because the annual distance is higher. Data values for Fig. 3 are 2.78; 9.18; 11.57; 11.25;

10.59; 9.16; 7.72; 5.93; 5.37; 4.5; 4.14; 2.72; 2.96; 2.13; 2.28; 1.22; 1.3; 1.38; 0; 0; 1.62.

TABLE IV: ANNUAL EQUIVALENT FULL CYCLES

Number of days N_d	Driving distance per day D_{ad} (km)	Number of charging per day N_{charge}	Charge limits (km)	Annual equivalent full cycles N_{acd}
71	8	1	25	2.78
78	24	1	25	9.18
59	40	1	50	11.57
41	56	1	75	11.25
30	72	1	75	10.59
21	89	1	100	9.16
15	105	2	75	7.72
10	121	2	75	5.93
8	137	2	75	5.37
6	153	2	100	4.50
5	169	2	100	4.14
3	185	2	100	2.72
3	201	3	75	2.96
2	217	3	75	2.13
2	233	3	100	2.28
1	249	3	100	1.22
1	266	3	100	1.30
1	282	3	100	1.38
1	330	4	100	1.62

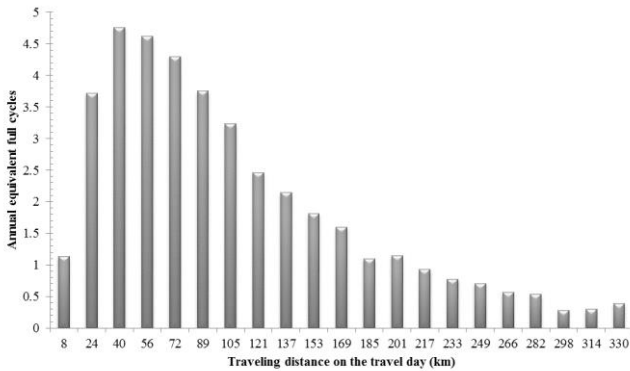


Fig. 3. Annual equivalent full cycles divided into annual traveling categories.

Annual driving distance can be calculated as

$$D_{ad} = \sum(N_d \times D_{ad}). \quad (2)$$

Values from Table IV provided 19,954 km for annual driving distance; a total number of days is 358 because values are rounded to integers. This distance arrived from real driving data.

IV. BATTERY MEASUREMENTS FOR A123 SYSTEMS' ANR26650M1-A™

The wearing of battery cell a) decreases battery capacity, b) increases inner resistance, c) increases power loss and d) causes a variation in impedance spectra. The wearing of a battery cell is influenced by temperature, DoD, and charging and discharging power [5], [27]. The battery measurements were carried with the A123 Systems' ANR26650M1-A™ cylindrical cells in which the battery chemistry is composed of a LiFePO₄ cathode and a carbon anode. Nominal capacity for a battery cell is 2.2 Ah. Battery aging test results are shown in Table V [14]. The cut-off voltages were at 3.6 and

2.0 V. Tested temperatures were from -30 to 60 °C. DoD was from 10 to 90%. Current rates were 0.5It, 2It, 6It, and 10It. Our approach was to optimize lifetime and we neglected higher current rates 6It and 10It. Only 0.5It and 2It are shown in Table V. Current rate 0.5It correspond to 1 A and 2It corresponds to 4 A current. The battery cells were charged and maintained at 3.6 V before the electric current decreased under 0.1 A or maximum time of 48 hours was received [14]. Values in Table V either are the number of cycles in the ongoing or finalized test. For example, DoD 90%, temperature -30 °C, and It-rate 0.5It had two cells, which both survived only one cycle. The range at low temperature will be much smaller than the range at high temperature. That was not taken account in measurements; just the number of cycles was recorded.

TABLE V: NUMBER OF CYCLES FROM THE BATTERY CYCLE TEST. THE VALUES IN THE TABLE INDICATE THE NUMBER OF CYCLES ATTAINED BY THE BATTERY CELL

DoD (%)	-30 °C	0 °C	15 °C	25 °C	45 °C	60 °C	It-rate
90	1	2,242	2,144		1,796	754	0.5
	1	2,240	2,130		1,661	518	
80	1	2,520	2,390	2,439	2,120	1,011	0.5
	1	2,520	2,390	563	2,123	1,006	
50	13	3,976	3,827		3,387	3,355	0.5
	15	3,965	3,804		3,317	3,963	
20	2,662	9,625	9,234	4,711	8,374	9,801	0.5
	4,979	9,652		2,211	8,379	9,821	
0	9,678	18,579	18,067		16,235	19,098	0.5
	12,082	18,534	17,940		16,571	19,385	
90	26				4,492	1,276	2
	40				4,048	1,594	
80		2,249					2
		2,315					
		1,931					
		2,197					
50			3,532				2
			3,784				
			3,671				
			6,763				
10	38,733					54,934	2
	29,511					54,943	

Battery cell cycle tests for UR18650E™ was constructed with a temperature of 35 °C and the current rate of 1It [3]. To compare ANR26650M1-A™ tests to UR18650E battery cell tests, a temperature of 35 °C and the current rate of 1It was included in the investigation. Cycle numbers were calculated by using linear interpolation for the temperature of 35 °C and the current rate of 1It. Cycle numbers were calculated by using linear interpolation for DoD values 49, 37, 25, and 12%. Cycle numbers were 3,738; 5,834; 7,930; and 15,530. Multiplying DoD values and cycle numbers, we receive corresponding equivalent full cycles 1,832; 2,159; 1,982; and 1,864, respectively (TABLE VI). For a typical lithium-based battery, the cycle number per DoD tends to increase as the DoD decreases. In our case, cycle numbers per DoD were increasing 76; 158; 317; and 1294 as the DoD decreases 49, 37, 25, and 12%. That follows a typical lithium-based battery trend.

A. Charge Limits

Battery cell aging information was collected in Table VI.

Equivalent full cycles N_{cn} and used cycles N_{acm} were used for calculating battery cell lifetime aging N_l . Equivalent full cycles and used cycles in Table VI were collected from annual equivalent full cycles, as seen in TABLE IV. Four charge limits are limiting the range to 100, 75, 50, or 25 km. Range means maximum available driving distance and actual driving distance need to be smaller than range. For example, charge limit 1 is the longest range of 100 km and batteries will be charged every 100 km distance. With charge limit 1, we can receive 1,832 equivalent full cycles. When we sum all 100 km ranges equivalent full cycle values from Table IV, we receive numerical value for used cycles 28.33.

TABLE VI: CHARGE LIMITS, DISTANCES, EQUIVALENT FULL CYCLES, AND USED CYCLES FOR A123 SYSTEMS' ANR26650M1-A™ BATTERY CELLS

Charge limits	Distances (km)	Equivalent full cycles (N_{cn})	Used cycles (N_{acm})
1	100	1,832	28.33
2	75	2,159	45.95
3	50	1,982	11.54
4	25	1,864	11.96

B. Calculated Aging for Battery Cells

Battery cell lifetime aging (N_l) can be calculated using

$$N_l = \frac{\sum N_{acm}}{\sum N_{cn}}, \quad (3)$$

where N_{acm} is annual average equivalent full cycles and N_{cn} is equivalent full cycles.

Four charge limits' number values after calculation (3), generated 1,996 cycles, which when multiplied by 204 km, provided 407,151 km for a driving lifetime. This is far less than UR18650E battery driving lifetime of 2,742,000 km. Driving lifetime is surprisingly short for A123 Systems'™ cells. One of the reasons is low 240 km range for BYD e6™. Secondly, different measurement arrangements may cause a difference in driving lifetime. Notice that equivalent full cycle N_{cn} was calculated from the measured cycles. In other words, temperature, DoD, and It-rate are included in this value. The physical implication of (3) is transforming lifetime cycles from battery measurements to lifetime driving distance by help with vehicle range.

C. Lifetime Compensation for the V2G Process

The grid operator can choose a number of V2G cycles per day (N_c) according to the grid condition. The equations adapt driving patterns described in NHTS. To enhance battery life, the V2G process charging and discharging cycle was from 47.5% to 52.5% SoC, because the lowest battery cell degradation rate in aging tests was the one cycled between 47.5% and 52.5% SoC [3]. A number of V2G cycles per day (N_c) were transformed to annual equivalent full V2G cycles (N_{V2G}) by calculating

$$N_{V2G} = \frac{N_c \times 5}{100} \times 365 \quad (4)$$

where N_c is the chosen V2G cycles per day.

The EES varied V2G cycles between 0 and 50. The calculations in this manuscript were based on 24 V2G cycles per day. Equivalent full V2G cycles per year (N_{V2G}) for the

V2G process were transformed into a driving distance (D_{ae}) by multiplying N_{V2G} by the driving range. If N_c is 24 V2G cycles, then the grid operator uses 24 V2G cycles from EV batteries. Because the lowest degradation rate in aging tests was the one cycled between 47.5% and 52.5% SoC [3], the nature of the V2G cycles is that battery management discharge batteries from 52.5% to 47.5% SoC and then recharge batteries up to 52.5% SoC. This is one V2G cycle. These cycles are repeated in this case 24 times per day.

The calculated V2G fraction (F_{V2G}) is a relation between V2G cycles and maximum available cycles (N_{c2})

$$F_{V2G} = \frac{N_{V2G}}{N_{c2}}, \quad (5)$$

where N_{c2} is equivalent full cycles with a charge limit of four.

Charge limit 2 was used for V2G regulation because it has the largest number of equivalent full cycles (2,159) as seen in Table VI. The physical implication of equation (5) was to show how large fraction of the total battery energy is provided for the V2G regulation.

The fraction of battery cell charge (F_{ad}), which was used for annual driving, is calculated from Table VI.

$$F_{ad} = \sum \frac{N_{acm}}{N_{cn}}, \quad (6)$$

where N_{acm} are cycles used for driving with four charge limits and N_{cn} is equivalent full cycles.

The physical implication of equation (6) was to show how large portion of the total battery energy is used for driving.

The V2G process reduces driving distance. The driving distance reduction (D_{ar}) can be calculated as

$$D_{ar} = \frac{D_{ad}}{F_{ad}} \times F_{V2G}, \quad (7)$$

where D_{ad} is the EV driving distance per year from equation (2), F_{ad} is the fraction of EV battery charge used for driving from equation (6) and F_{V2G} is a fraction of V2G cycles.

The physical implication of equation (7) was to show how much the V2G process degrades the EV batteries.

After the V2G process reduction, we calculated battery life as a driving distance with an optimal charging schedule

$$D_{ld} = \frac{D_{ad}}{F_{ad} + F_{V2G}}. \quad (8)$$

In this case, we obtained a driving distance of 79,209 km. Our result articulates that the longest driving distance before batteries need to change is 79,209 km. Battery cells have reduced driving distance with V2G usage.

The cycle life of the EV batteries (T_l) can be calculated by equation (9)

$$T_l = \frac{D_{ld}}{D_{ad}}. \quad (9)$$

In this example, lifetime value (T_l) was 4 years. Our result suggests life cycle, not the calendar life of the EV batteries. These lifetimes are ideal cycle lifetimes with optimized charging patterns and V2G cycles. Calendar life is giving a limit to the lifetime, which was not included in this study.

The distance reduction during the lifetime (D_{lr}) explains how much the V2G process consume the battery life, which can be calculated by using equation (10)

$$D_{lr} = D_l - D_{ld} , \quad (10)$$

where D_l is maximum driving distance during a lifetime without the V2G process and D_{ld} is driving distance during a lifetime with the V2G process from equation (8).

The grid operator receives benefits from the V2G process and compensates battery cell degradation to the EV battery owner. The V2G compensation during the lifetime (P_{lc}) can be calculated by using equation (11)

$$P_{lc} = \frac{D_{lr}}{D_l} \times P_b , \quad (11)$$

where P_b is the purchase price of the EV battery.

The estimated battery purchase price was AU\$ 16,640.

We can calculate the annual compensation of battery wear (P_{ac}) for the V2G process using the equation (12):

$$P_{ac} = \frac{D_{ar}}{D_l} \times P_b . \quad (12)$$

As a result, annual V2G compensation P_{ac} for ANR26650M1-A™ cells were calculated at AU\$ 2,983, which grid operators compensate because of battery wear. For that investment, grid operators receive 24 V2G cycles a day to support power grid balance. If the number of V2G cycles N_c is 12, the annual grid operators compensation is cut in half to AU\$ 1,491. Therefore, the grid operator needs to pay more for the V2G use if numbers of V2G cycles are increased. As a result, as the point of grid operators view ANR26650M1-A™ cells are not attractive for V2G process.

The annual energy (E_{V2G}) transferred because of the V2G process can be calculated by equation (13)

$$E_{V2G} = \frac{E_b \times 5}{100} \times N_c \times 365 , \quad (13)$$

where E_b is EV battery capacity.

Annual energy (E_{V2G}) for A123 Systems™ cells was calculated at 32,850 kWh, meaning 90 kWh per day. This energy is cycled between battery and power grid. We calculate the electricity price (P_{kWh}), which is used for the V2G process

$$P_{kWh} = \frac{P_{ac}}{E_{V2G}} \quad (14)$$

Electricity price (P_{kWh}) for A123 Systems™ cells was calculated at 9.08 cents per kWh. Power grid uses the V2G process for frequency regulation. When power grid frequency is low, batteries inject electricity to the power grid. Accordingly, when the power grid frequency is high, the power grid returns electricity recharge back to the batteries. The grid operator needs to pay a relatively low energy price for the use of Sanyo UR18650E™ cells.

Annual V2G compensation (P_{ac}) from equation (12) is combined from equations (2), (4), (6) and (7).

$$P_{ac} = \frac{\sum_{n=1}^{19} (N_d \cdot D_{ad})_n \cdot N_c \cdot 5 \cdot 365 \cdot P_b}{100 \cdot N_{cn} \sum_{n=1}^4 (N_{acm})_n \cdot D_{range}} . \quad (15)$$

The sensitivity test determines the relative significance of each of the input variables. The sensitivity of variables in equation (15) was calculated by multiplying every variable by number 10. The change in output (P_{ac}) was compared to the input variable.

$$S = \frac{\Delta Output}{\Delta Input} \times 100 \quad (16)$$

Sensitivity values were as follows:

D_{ad}	D_{range}	N_{acm}	N_c	N_{c2}	P_b
100.03	0	-90.93	100.03	-90.86	99.95

Fig. 4 shows sensitivity levels. Columns are nearly the same size. Positive columns increase annual V2G compensation and negative columns decrease annual V2G compensation. Annual distance drove (D_{ad}), number of V2G cycles (N_c), and battery package cost (P_b) increase annual V2G compensation. Equivalent full cycles per year (N_{acm}) and V2G charge limit (N_{c4}) decrease annual V2G compensation. Range (D_{range}) do not affect annual V2G compensation.

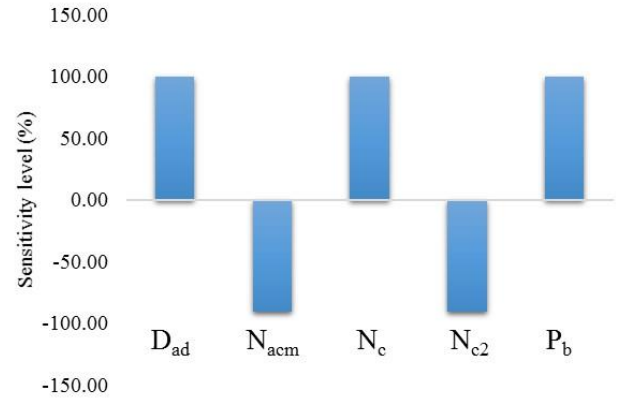


Fig. 4. Sensitivity levels for annual distance drove (D_{ad}), equivalent full cycles per year (N_{acm}), number of the vehicle to grid cycles (N_c), and equivalent full cycles in the vehicle to grid charge limit (N_{c4}) and battery package cost (P_b).

V. RESULTS FOR A123 SYSTEMS' ANR26650M1-A™ LiFePO₄ CELLS AND SANYO'S UR18650E™ Li(NiMnCo)O₂ CELLS

Battery aging tests are carried for Sanyo's UR18650E™ Li(NiMnCo)O₂ cells [3]. V2G cycles are carried nearby 50% SoC. The battery capacity is 2.05 Ah and the electric current rate is 1It, which suggest 2.05 A electric current. Curves in Fig. 5 illustrates that the lower battery cycle depth provides a longer battery life. To enhance EV battery life, cycle depths 5, 10, 15, and 20% are selected as charge limits.

The longest lifetime distance D_{ld} for UR18650E battery cells was 372,462 km. The lifetime value T_l for UR18650E cells was 18.27 years. The annual V2G compensation P_{ac} for UR18650E battery cells with 24 V2G cycles was AU\$ 770. The energy E_{V2G} for Sanyo's™ cells is 37,230 kWh a year and 102 kWh a day. V2G operations transfer electricity between the grid and EV batteries. V2G operations energy

price P_{kWh} for Sanyo's™ cells is calculated at 2.08 cents per kWh [10].

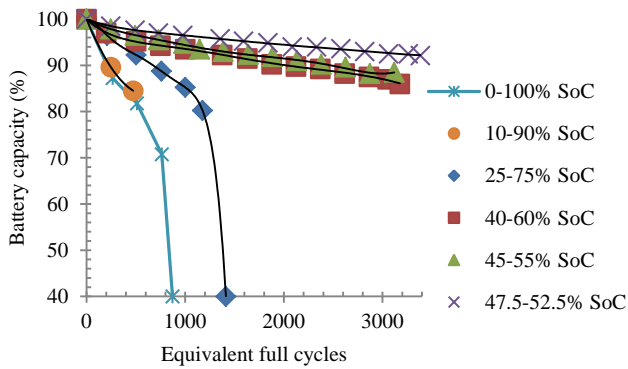


Fig. 5. Measurement results for battery capacity against equivalent full cycles. Battery cell cycles around a mean State of Charge (SoC) of 50% are compared.

LiFePO₄ and Li(NiMnCo)O₂ battery technologies are compared in terms of durability when used in vehicle to grid operations. Equivalent full cycles are shown in Fig. 6. The A123 Systems™ cells cycle depths are DoD and for Sanyo™ cells cycle depths the average capacity is 50%. For example, 5% cycle depth for A123 Systems™ cells were cycled between 95 and 100% and for Sanyo™ cells, 5% cycle depth were cycled between 47.5 and 52.5% SoC. Comparison between these cells is difficult especially in low cycle depths as seen in Fig. 6. For Sanyo's™ batteries, the lowest cycling depth provides the longest lifetime. For A123 Systems™ batteries, DoD seems to have a negligible lifetime. For Sanyo's™ batteries, lifetime clearly increases when cycling depth is under 50%. The longest lifetime, 9,461 equivalent full cycles, was reached when cycling depth is 5%. It is almost a nine times longer lifetime compared to A123 Systems™ batteries 1,071 equivalent full cycles when DoD is 5%. When the range is 500 km, 5% means charging every 25 km. These low cycling depth values are possible if a battery pack is large enough. Using only a 5% fraction of the battery capacity, the lifetime can be increased up to 9,461 x 500 km, which brings 4.7 million km. This high lifetime can be achieved if charging is done every 25 km or more frequently, and the range needs to be large. If the range is small, charging is made using high DoD. In high DoD, A123™ batteries have a longer lifetime than Sanyo™ batteries. This is why Sanyo's™ cells are suitable for EV with large battery capacity and A123 Systems™ cells for small capacity EV application. LiFePO₄, although known as a long-life battery, suffers from more severe degradation under shallow cycles than Li(NiMnCo)O₂. Controlled and uncontrolled charging brings similar lifetime expectancy for LiFePO₄ cells. This provides more freedom also V2G operation when a large amount of power can be transferred to the power grid. Controlled and uncontrolled charging brings obvious difference for Li(NiMnCo)O₂ cells. SoC window should be strictly limited near 50% SoC area limiting the amount of transferred power. To elucidate the findings in Fig. 6, Sanyo™ cells do not wear out in V2G operation, because available equivalent full cycles are 9,461. When multiplied by 20 we receive 189,220 V2G cycles during a lifetime.

In the data of TABLE V obtained from the actual

experiment of LiFePO₄ type, it can be seen that as the DoD is lowered at the same It-rate, the cycle tends to increase, but Fig. 6 does not. In the case of A123 systems™, even though the LiFePO₄ battery is used, the result is flat. With such a graph, it can be seen that the flat LiFePO₄ type, does not affect the deterioration even if the charge/discharge is deep with a low capacity. Noticeable, TABLE V shows cycle numbers; however, Fig. 6 shows equivalent full cycles. For example, linear extrapolation for 35 °C temperature, 1It current rate and 10% DoD provides 17,202 cycles. Only 10% of energy is used and equivalent full cycles are 1,071 cycles.

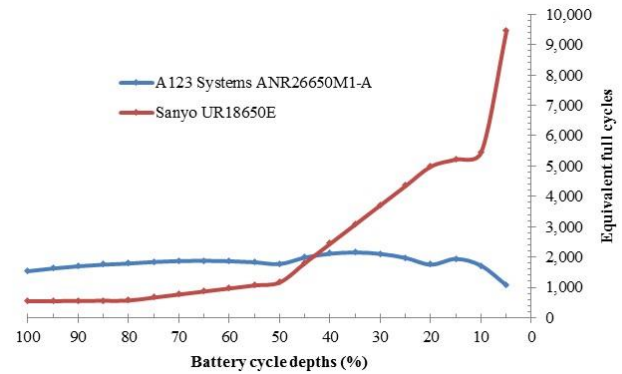


Fig. 6. Equivalent full cycles for two different Li-ion batteries. The A123 Systems™ cells cycle depths are depths of discharge and for Sanyo™ cells cycle depths the average capacity is 50%.

In the V2G application, battery cells should have high equivalent full cycles. Sanyo™ cells have the highest equivalent full cycles when cells are cycled between 47.5 and 52.5% SoC [3]. To develop batteries for the V2G application, equivalent full cycles should be higher. Evaluation of battery life in the V2G application should be focused on improving the cell performances in equivalent full cycle area.

The number of V2G cycles affects the lifetime of the EV battery. A123 Systems™ batteries lifetime curves are shown in Fig. 7. A number of V2G cycles and battery size affect the battery lifetime. For example, 24 V2G cycles per day and 75 kWh batteries provide four years' battery cell lifetime.

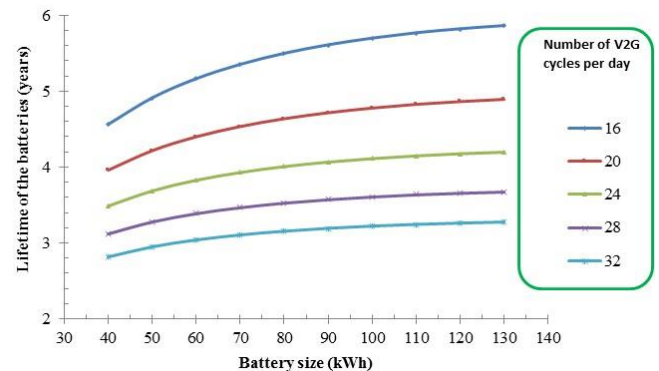


Fig. 7. A lifetime of the batteries for ANR26650M1-A™ LiFePO₄ battery cells.

The contour plot shows a lifetime for A123 Systems™ ANR26650M1-A™ LiFePO₄ battery cells in Fig. 8 (a). A lifetime of four years can be read when the battery size was 75 kWh and 24 V2G cycles were used per day. The longest lifetime, 5.56 years, was reached with a low number of V2G cycles and with large battery size. A123 Systems™ cells are

not sensitive to DoD, but life remains short. The strongest indicator of battery capacity fade is the processed battery energy, not DoD [1]. The contour plot shows that battery size is not an important factor, however number of V2G cycles degrade battery lifetime noticeably. From this contour plot, we can choose the desired battery cell cycle life and read according to battery size and V2G numbers. In EES software, battery size, number of V2G cycles, and lifetime are parameters in the parametric table. The EES use equation (9) to plot Fig. 8.

Another contour plot shows a lifetime for Sanyo's UR18650E™ Li(NiMnCo)O₂ cells in Fig. 8 (b). Lifetimes are clearly longer for UR18650E than ANR26650M1-A battery cells. UR18650E lifetimes are long enough for EV use with battery size 85 kWh and 24 V2G cycles per day, providing 18.27 years lifetime for battery cells. Increasing battery size lifetime was increased and increasing V2G cycles per day lifetime were decreased.

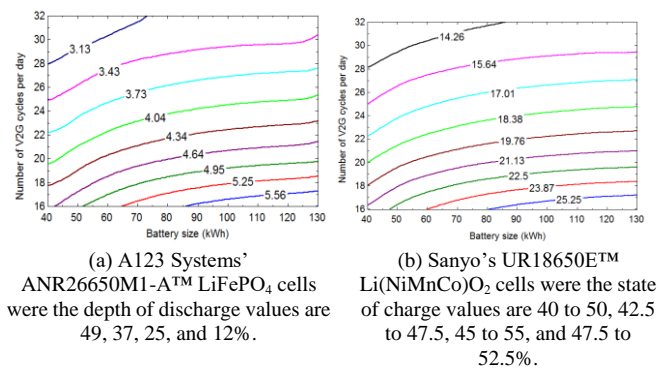


Fig. 8. A lifetime of the batteries in years. Contour plots from two measurements.

VI. INTERPRETATION AND DISCUSSION

In V2G operations, electricity is flowing from the electricity network to the batteries and from the batteries back to the electricity network. Using direct real-time control of the grid operator, battery charger charges batteries, providing V2G balance and frequency regulation to the grid. As smart charging is an important part of EV penetration, V2G may provide an important extension for smart charging procedures. For satisfying the scheduled charging, we propose to switch the V2G control to a smart charging control. EV batteries can be utilized as battery storage as a flexible distributed energy resource [28]. Energy management mitigates the dependency on the power grid and supply power according to electrical load and price trend [29]. Balancing electrical load mitigate the power grid fluctuations due to synchronization of V2G operations [30]. The V2G concept is considered as an extension of the smart charging system allowing EVs to be able to inject electricity into the electricity network, acting as distributed generators or battery storage systems.

One of the merits of this research is providing information for V2G battery selection. V2G reduces the lifetime of the batteries. Degradation is reduced by choosing an optimal charging window SoC. In Sanyo™ batteries, 47.5 to 52.5% SoC shows prolonged lifetime and is suitable for V2G operations. One V2G cycle is 47.5 to 52.5% SoC and covers 5% window of battery capacity. Such a V2G cycle does not

affect much a lifetime. The battery model uses 24 V2G cycles; every cycle is 5% slide from the battery capacity. Battery life consists of calendar life and cycle life. Calculated cycle life 18.27 years means numbers of cycles. If calendar life is lower than cycle life, the user can increase V2G cycles to receive more income. The total life is either calendar life or cycle life, which comes earlier.

Low charge level is avoided because usually empty batteries are thought to have accelerated aging. However, Sanyo™ battery measurements show that prolonged calendar life is received with empty batteries. That seems to be in conflict with cycle life measurements. We just need to accept that battery cell degradation behavior is different in calendar life test from cycle life test.

The vehicle information was from BYD e6™ battery electric vehicle. The range was 204 km and the battery capacity was 75 kWh. Battery cells were the A123 Systems' ANR26650M1-A™ LiFePO₄ cells. The electric charge for these 26650 cylindrical cells was 2.2 Ah. Results were compared to Sanyo's UR18650E™ Li(NiMnCo)O₂ cells. Vehicle information initial values were from the Tesla Model S™ BEV. The range was 500 km and battery capacity was 85 kWh. These choices made a connection to real-life as these batteries are used in EV configuration. However, the range performance of these vehicles are in a different category and affected results. This is good to keep in mind when using this information for V2G battery selection.

In the data obtained from the actual experiment of LiFePO₄ type, it can be seen that as the DoD is lowered at the same It-rate, the cycle tends to increase, but equivalent full cycles do not. In case of an A123 system™, even though the LiFePO₄ battery is used, the result is flat. With such a result, it can be seen that the flat LiFePO₄ type does not affect the deterioration even if the charge/discharge is deep with a low capacity. However, in reality, this is not likely. Original cycle numbers have fluctuation, which may cause flat lifetime prediction. Usually, lifetime prediction looks like Li(NiMnCo)O₂ cell prediction showing prolonged lifetime in 47.5 to 52.5% SoC area. Surprisingly LiFePO₄ type cell did not show the same pattern. With new test arrangements, we suppose that both battery cell chemistries will show similar degradation pattern.

VII. CONCLUSION

Principal findings are lifetime reduction is decreased in V2G operations and a lifetime can be extended. Optimal window of SoC was used in V2G operations and selected SoC windows are used in driving use. This study is important to the community and is worthy of note because it shows an extended lifetime with battery management instead of developing battery chemistry. Implications of the findings are the importance of battery management system in V2G operations and V2G operations will become more compelling technology. The research, as well as the findings, have addressed the defined objective by degreasing lifetime influence from V2G operations.

Battery cell wearing was compared between A123 Systems' ANR26650M1-A™ LiFePO₄ cells and Sanyo's UR18650E™ Li(NiMnCo)O₂ cells. The author concludes that Sanyo's™ cells are suitable for EV with large battery

capacity and A123 SystemsTM cells for small capacity EV application. The explanation is that with large battery capacity, only a small fraction of battery capacity is used for driving. With a small battery capacity, a full charge and discharge are needed frequently. The difference between Sanyo'sTM cells and A123 SystemsTM cells lifetimes was significant. Lifetime was calculated at four years for A123 SystemsTM cells and 18.27 years for Sanyo'sTM cells. The cycle lifetime difference was caused by different measurement methods. The annual V2G cost was higher for A123 SystemsTM cells than for Sanyo'sTM cells. V2G operations provide frequency regulation and balancing power for the power grid. Energy used for V2G operations is 90 kWh a day for A123 SystemsTM cells and for Sanyo'sTM cells 102 kWh per day. The life cycle of the Li(NiMnCo)O₂ is 9 times more than that for the LiFePO₄ at 5% cycle depths. Energy price is 9.08 cents per kWh for A123 SystemsTM cells and 2.07 cents per kWh for Sanyo'sTM cells. This means that the energy price for A123 SystemsTM cells was four times more expensive than for Sanyo'sTM cells. If the battery charge is always held near 50%, the lifetime can be extended for Li(NiMnCo)O₂ battery cells. A123 SystemsTM cells were fully charged and do not show if a similar phenomenon around 50% is possible. However, if both cells are fully charged and fully discharged, A123 SystemsTM cells last longer than Sanyo'sTM cells.

Battery cycle aging measurement was carried in a different way. That causes uncertainty for comparison. Available data were not successfully compared to each other. Both investigated cells can be simulated with different parameters and optimized cycle life was used here. However, results can be used for optimizing battery cycle life in V2G use, not for comparison. The used approach cannot be used as a comparison, only for a separate investigation. Future work includes more studies to make a comparison in a satisfactory manner, where different batteries have different lifetime equations. In the future improvement of the battery model, we should construct the lifetime equation according to battery cell type.

APPENDIX A: NOMENCLATURE

Variable	Variable definition	Value used
N_{acd}	Annual equivalent full cycles	1.22 to 11.57 cycles
D_{dd}	Distance drove per day	8 to 330 km
D_{range}	Maximum driving distance per one charge	204 km
N_d	Number of days	1 to 71 days
D_{ad}	Annual driving distance	19,954 km
N_l	Battery lifetime wearing	1996 cycles
N_{acm}	Used cycles, all charge limits	11.57 to 45.95 cycles
N_{cn}	Lifetime equivalent full cycles	1,832 to 2,982 cycles
N_{V2G}	Annual equivalent full V2G cycles	438 cycles
D_{ae}	Annual equivalent V2G distance	89,352 km
N_c	Number of V2G cycles per day	24 cycles
F_{V2G}	The fraction of V2G cycles to the maximum number of cycles	0.202908363
N_{c2}	Equivalent full cycles, charge limit two	2,159 cycles
F_{ad}	The fraction of battery capacity for driving	0.049008882
D_{ar}	Annual V2G distance reduction	82,614 km

D_{ld}	Lifetime driving distance with V2G operations	79,209 km
T_l	A lifetime of the batteries	4 years
D_{tr}	Reduction of distance because of V2G operations	327,942 km
D_l	Lifetime driving distance	407,151 km
P_{lc}	Lifetime compensation for V2G usage	\$11,841
P_b	Estimated battery package cost	\$14,701
P_{ac}	Annual V2G compensation	\$2,983
E_{V2G}	Annual energy used for V2G	32,850 kWh
E_b	Battery energy capacity	75 kWh
P_{kWh}	Energy price used for V2G	9.08 c/kWh

REFERENCES

- [1] S. B. Peterson, J. Apt, and J. Whitacre, "Lithium-ion battery cell degradation resulting from realistic vehicle and vehicle-to-grid utilization," *Journal of Power Sources*, vol. 195, no. 8, pp. 2385-2392, 2010.
- [2] D. Anseñ et al., "Operando lithium plating quantification and early detection of a commercial LiFePO₄ cell cycled under dynamic driving schedule," *Journal of Power Sources*, vol. 356, pp. 36-46, July 2017.
- [3] M. Ecker et al., "Calendar and cycle life study of Li(NiMnCo)O₂-based 18650 lithium-ion batteries," *Journal of Power Sources*, vol. 248, pp. 839-851, Feb. 2014.
- [4] M. Ecker et al., "Development of a lifetime prediction model for lithium-ion batteries based on extended accelerated aging test data," *Journal of Power Sources*, vol. 215, pp. 248-257, 2012.
- [5] J. Vetter et al., "Ageing mechanisms in lithium-ion batteries," *Journal of Power Sources*, vol. 147, no. 1, pp. 269-281, 2005.
- [6] X. Li, J. Jiang, L. Y. Wang, D. Chen, Y. Zhang, and C. Zhang, "A capacity model based on charging process for state of health estimation of lithium ion batteries," *Applied Energy*, vol. 177, pp. 537-543, Sep. 1, 2016.
- [7] B. Xu, A. Oudalov, A. Ulbig, G. Andersson, and D. Kirschen, "Modeling of lithium-ion battery degradation for cell life assessment," *IEEE Transactions on Smart Grid*, vol. 9, no. 2, pp. 1131-1140, 2016.
- [8] M. Petit, E. Prada, and V. Sauvant-Moynot, "Development of an empirical aging model for Li-ion batteries and application to assess the impact of Vehicle-to-Grid strategies on battery lifetime," *Applied Energy*, vol. 172, pp. 398-407, June 15, 2016.
- [9] L. C. Casals, B. A. Garca, F. Aguesse, and A. Iturrondobeitia, "Second life of electric vehicle batteries: relation between materials degradation and environmental impact," *The International Journal of Life Cycle Assessment*, vol. 22, no. 1, pp. 82-93, 2017.
- [10] T. Lehtola and A. Zahedi, "Cost of EV battery wear due to vehicle to grid application," presented at the Power Engineering Conference (AUPEC), 2015 Australasian Universities, Wollongong, New South Wales, Australia, 27-30 Sept., 2015.
- [11] S. Kabitzi et al., "Cycle and calendar life study of a graphite|LiNi 1/3 Mn 1/3 Co 1/3 O 2 Li-ion high energy system. Part A: Full cell characterization," *Journal of Power Sources*, vol. 239, pp. 572-583, 2013.
- [12] T. Guan et al., "The effect of elevated temperature on the accelerated aging of LiCoO₂/mesocarbon microbeads batteries," *Applied Energy*, vol. 177, pp. 1-10, Sep. 1, 2016.
- [13] L. W. Juang, P. J. Kollmeyer, A. E. Anders, T. M. Jahns, R. D. Lorenz, and D. Gao, "Investigation of the influence of superimposed AC current on lithium-ion battery aging using statistical design of experiments," *Journal of Energy Storage*, vol. 11, pp. 93-103, June 1, 2017.
- [14] J. Wang et al., "Cycle-life model for graphite-LiFePO₄ cells," *Journal of Power Sources*, vol. 196, no. 8, pp. 3942-3948, 2011.
- [15] Z. Mhadhbi, C. Gueguen, S. Zairi, and B. Zouari, "Autonomous distributed energy management for intelligent microgrids," *Journal of Clean Energy Technologies*, vol. 6, no. 1, pp. 31-40, Jan. 2018.
- [16] E. Sarasketa-Zabala, E. Martinez-Laserna, M. Berecibar, I. Gandiaga, L. M. Rodriguez-Martinez, and I. Villarreal, "Realistic lifetime prediction approach for Li-ion batteries," *Applied Energy*, vol. 162, pp. 839-852, Jan. 1, 2016.
- [17] M. Swierczynski, D. I. Stroe, A. I. Stan, R. Teodorescu, and S. K. Kær, "Lifetime estimation of the Nanophosphate LiFePO₄/C Battery chemistry used in fully electric vehicles," *IEEE Transactions on Industry Applications*, vol. 51, no. 4, pp. 3453-3461, 2015.
- [18] Y. Zhang, C. Y. Wang, and X. Tang, "Cycling degradation of an automotive LiFePO₄ lithium-ion battery," *Journal of Power Sources*, vol. 196, no. 3, pp. 1513-1520, 2011.

- [19] K. Liu, J. Wang, T. Yamamoto, and T. Morikawa, "Modelling the multilevel structure and mixed effects of the factors influencing the energy consumption of electric vehicles," *Applied Energy*, vol. 183, pp. 1351-1360, Dec. 1, 2016.
- [20] D. Aurbach, B. Markovsky, Y. Talyossef, G. Salitra, H. J. Kim, and S. Choi, "Studies of cycling behavior, ageing, and interfacial reactions of LiNi_{0.5}Mn_{1.5}O₄ and carbon electrodes for lithium-ion 5-V cells," *Journal of Power Sources*, vol. 162, no. 2, SPEC. ISS., pp. 780-789, 2006.
- [21] S. Barcellona, M. Brenna, F. Foadelli, M. Longo, and L. Piegari, "Analysis of ageing effect on Li-polymer batteries," *The Scientific World Journal*, 2015.
- [22] S. Brown *et al.*, "Cycle life evaluation of 3 Ah Li_xMn₂O₄-based lithium-ion secondary cells for low-earth-orbit satellites. I. Full cell results," *Journal of Power Sources*, vol. 185, no. 2, pp. 1444-1453, 2008.
- [23] J. R. Belt, C. D. Ho, T. J. Miller, M. A. Habib, and T. Q. Duong, "The effect of temperature on capacity and power in cycled lithium ion batteries," *Journal of Power Sources*, vol. 142, no. 1-2, pp. 354-360, 2005.
- [24] A. Zeh, M. Müller, M. Naumann, H. C. Hesse, A. Jossen, and R. Witzmann, "Fundamentals of using battery energy storage systems to provide primary control reserves in Germany," *Batteries*, vol. 2, no. 3, p. 29, 2016.
- [25] C. Guenther, B. Schott, W. Hennings, P. Waldowski, and M. A. Danzer, "Model-based investigation of electric vehicle battery aging by means of vehicle-to-grid scenario simulations," *Journal of Power Sources*, vol. 239, pp. 604-610, Oct. 1, 2013.
- [26] A. Santos, N. McGuckin, H. Y. Nakamoto, D. Gray, and S. Liss, "Summary of travel trends: 2009 National Household Travel Survey (NHTS)," in *Trends in Travel Behavior, 1969-2009*, Washington, DC, USA FHWA-PL-II-022 2011.
- [27] M. Broussely *et al.*, "Main aging mechanisms in Li ion batteries," *Journal of Power Sources*, vol. 146, no. 1-2, pp. 90-96, Aug. 26, 2005.
- [28] G. Mills and I. MacGill, "Assessing electric vehicle storage, flexibility, and distributed energy resource potential," *Journal of Energy Storage*, vol. 17, pp. 357-366, 06/01/ 2018.
- [29] L. Han, Z. Jianhua, and S. Rafique, "Implementation of battery management module for the microgrid: A case study," *International Journal of Smart Grid and Clean Energy*, vol. 6, no. 1, pp. 11-20, 2017.
- [30] T. Nagata and S. Monde, "A multi-agent based micro-grid operation method considering charging and discharging strategies of electric vehicles," *International Journal of Smart Grid and Clean Energy*, vol. 8, no. 2, pp. 149-155, 2019.



Timo A. Lehtola is born in Finland and holds a master's degree in Energy Technology from the Lappeenranta University of Technology and a master's degree in physics from the University of Helsinki.

He is a Ph.D. student at the James Cook University, Australia. Previous publications include a review article in *Sustainable Energy Technologies and Assessments* in 2019, titled "Solar energy and wind power supply supported by storage technology: A review". Previous research interests include battery management and peak demand management in grid-connected electric vehicles and distributed renewable energy generation systems.

Mr. Lehtola is a member of IEEE, IEEE Young Professionals, Cigré CigréNext Generation Network, and IEEE Power & Energy Society. He has received IEEE PES Queensland Travel Award in 2016.



Ahmad Zahedi is an associate professor, and he is with the college of Science, Technology, and Engineering of James Cook University, Queensland, Australia.

Educated in Iran and Germany, Ahmad is author or co-author of more than 180 publications including 4 books and has trained 20 postgraduate candidates at Ph.D. and master levels, has examined more than 50 Ph.D. and Master Thesis, and completed 15 research and industry-funded projects. Ahmad has 26 years tertiary teaching and research and 6 years industry experience.